Construction and Building Materials 228 (2019) 116752

Contents lists available at ScienceDirect

Construction and Building Materials

journal homepage: www.elsevier.com/locate/conbuildmat

Effect of sulfate ions on corrosion of reinforced steel treated by DNA corrosion inhibitor in simulated concrete pore solution

Chen Chen, Linhua Jiang *, Ming-Zhi Guo, Peng Xu, Lei Chen, Jie Zha

College of Mechanics and Materials, Hohai University, Nanjing 210098, PR China

HIGHLIGHTS

- Effect of DNA inhibitor on chloride-induced steel corrosion under SO_4^{2-} was studied.
- The corrosion inhibition mechanisms were dissected by linear polarization and EIS.
- XPS was performed to examine surface membrane on steel electrode.

ARTICLE INFO

Article history:
Received 31 January 2019
Received in revised form 8 July 2019
Accepted 16 August 2019
Available online 24 August 2019

Keywords:
Sulfate ions
DNA corrosion inhibitor
Simulated concrete pore solutions
Electrochemical method
Corrosion

ABSTRACT

In this paper, a mixture of primers with a length of 20–80 bases were dissolved in a nucleic acid buffer as a deoxyribonucleic acid (DNA) corrosion inhibitor. The effect of coexisting anion SO_4^{2-} on the corrosion inhibition of DNA on the chloride-induced corrosion of reinforced steel in simulated concrete pore solution was studied by linear polarization and electrochemical impedance spectroscopy (EIS). The structure of the surface membrane of steel electrode after different treatments was analyzed using X-ray photoelectron spectroscopy (XPS). The results showed that the presence of SO_4^{2-} in the Cl^- abundant environment adversely reduced the corrosion inhibitor efficiency of the DNA corrosion inhibitor. Interestingly, with the increase of NaCl concentration, the effect of SO_4^{2-} on the corrosion resistance of DNA corrosion inhibitor and commercial corrosion inhibitor was smaller and less. More importantly, the efficiency of the adopted DNA corrosion inhibitor was higher than that of the typical commercial corrosion inhibitor (sodium phosphate) under the same condition. Findings from this study may provide new insights into the use of environmentally-friendly corrosion inhibitor in reinforced concrete structures and their performance in the presence of sulfate ions.

1. Introduction

Concrete is by far the most widely used construction engineering materials due to its low price and long durability. However, plain concrete suffers from low tensile and flexural strength, as well as brittleness. In real applications, steel has been predominantly embedded in concrete to form reinforced concrete. By far, reinforced concrete structures hold the greatest share of common structural forms worldwide. However, in marine and de-icing environments, chloride-induced corrosion of the reinforced concrete is a big concern [1–8]. Moreover, the widespread presence of oceans, saline-alkali lands and brine in salt lakes also provides a rich source of chloride ions for the corrosion of the reinforced steels in concrete [9–11]. With the continuous migration of ions into the reinforced concrete structures, the corrosion of reinforced steels can cause cracks in a short period [12], which not only endangers the safety of the structure but also brings huge economic losses [13]. Thus, reducing or even eliminating the corrosion of reinforced concrete in such aggressive environments is of great significance.

A wide range of methods have been employed to reduce the corrosion of reinforced steel, such as using improved materials (stainless steel), cathodic protection, realkalization, steel coating, use of corrosion inhibitors, etc. [14–16]. Among all the available techniques, the use of corrosion inhibitors represents one of the most practical methods due to its ease of operation, low cost and effective corrosion inhibition [17]. Based on the mechanism of action, corrosion inhibitors can be divided into two types: anode type and cathode type. Anodic corrosion inhibitors (typically, chromate, nitrite and molybdate) can prevent or slow down the anodic process by means of forming "protective films" on the surface of reinforced steels. For example, nitrite has been widely used as

* Corresponding author.
E-mail address: lhjiang@hhu.edu.cn (L. Jiang).

https://doi.org/10.1016/j.conbuildmat.2019.116752
0950-0618/

the main component of corrosion inhibitors in the early stage because of its excellent corrosion inhibiting effect. However, the downside of the nitrite inhibitor is that local corrosion and accelerated corrosion will occur when the concentration of chloride ions reaches a certain level. Thus, it earns the name of dangerous corrosion inhibitor [18,19]. In addition, nitrite inhibitor is infamous for carcinogenic alkali aggregate reaction, which significantly affects the slump. Therefore, its use as corrosion inhibitor is quite limited.

On the other hand, cathodic corrosion inhibitors, such as zincate, phosphate and organic compounds, prevent or slow down the cathodic process by means of forming a passive film via adsorption [20]. Most of cathodic corrosion inhibitors are not effective when used alone. Thus, a mixture of different types of corrosion inhibitors (normally, a reasonable combination of cathode type, anode type, increasing resistance type, reducing oxidation type and other substances) has been adopted. Such mixing corrosion inhibitors have good rust resistance and low toxicity. But the synthesis method and process are complicated. Moreover, corrosion inhibitors are mostly introduced to the concrete matrix by the intermixing method. The addition of a large amount of a mixture of different types of corrosion inhibitors cannot guarantee a uniform distribution of each type on the surface of steel [21]. Recently, DNA corrosion inhibitor has been identified as a good antirust candidate, which holds several advantages over conventional corrosion inhibitors, such as environmentally-friendly nature, long action time, simple and synthesis method. Therefore, it holds great promise for broad applications [22,23].

China has hundreds of salt lakes, mainly distributed in Xinjiang, Inner Mongolia, Qinghai, and Tibet. The salt content of brine in these salt lakes can be 5–10 times higher than that of seawater, mainly including chlorine salt and myriad sulfate salts (such as potassium, sodium and magnesium sulfates) [24]. Hence, reinforced concrete structures implemented in these areas are subjected to a combination of destructive effects caused by chloride ions and sulfates. At present, however, most previous studies focused on the corrosion behavior of reinforced concrete in chloride environments [25–32]. The few studies that have been undertaken in a coexistence of SO_4^{2-} and Cl^- environment only investigated the corrosion inhibition effect of conventional corrosion inhibitors reinforced concrete [33–35]. To the best of our knowledge, there is no study on the influence of sulfates on the corrosion inhibition of the environmentally-friendly nucleic acid corrosion inhibitors.

In this study, a mixed solution of deoxyribonucleic acids (DNA) of random sequences and with a length of 20 to 80 nucleotides was used as the corrosion inhibitor. Its corrosion inhibition effect on the steel was investigated in simulated concrete pore solutions prepared with both chloride and sulfate ions by means of linear polarization resistance and electrochemical impedance spectroscopy (EIS). The chemical compositions of passive films formed on the steel electrode in the DNA corrosion inhibitor solution was analyzed using X-ray Photoelectron Spectroscopy (XPS).

2. Experimental program

2.1. Preparation of reinforced steel

The carbon steel with a diameter of 10 mm was used in this study, and its chemical composition is shown in Table 1.

The cross sections of carbon steel rods with a length of 20 mm were polished by silicon carbide emery paper (grade 600). A copper wire was welded to the back of the working electrode, which was then embedded in epoxy resin with only one polished cross section exposed. The exposed surface had an area of 0.785 cm^2.

2.2. Preparation of simulated concrete pore solutions

The original DNA concentration was 615 ng/μL with DNA dissolved in DNA buffer. The chemical composition of DNA buffer was 10 mM Tris-Cl and 1 mM EDTA. The molecular structure of DNA is given in Fig. 1. Fig. 1(a) shows the molecular structure of a deoxynucleoside, in which B stands for one of the four bases: guanine (G), thymine (T), adenine (A), cytosine (C). Fig. 1(b) shows the molecular structure of an oligonucleotide. The DNA was single-stranded due to the high pH of saturated $Ca(OH)_2$ solution (about 12.5 at room temperature) [36]. Commercial phosphate corrosion inhibitor was used as a control.

Saturated $Ca(OH)_2$ solutions were prepared to simulate the concrete pore (SCP) solutions. To create different levels of sulfate contamination, 0.02, 0.05 and 0.10 mol/L Na_2SO_4 solutions were prepared. After 7 d of pre-passivation treatment, steel electrodes were soaked in SCP solutions without (blank) and with different

Table 1
Chemical composition of reinforced steel (wt. %).

C	Si	Mn	S	P
0.22	0.30	0.65	0.05	0.045

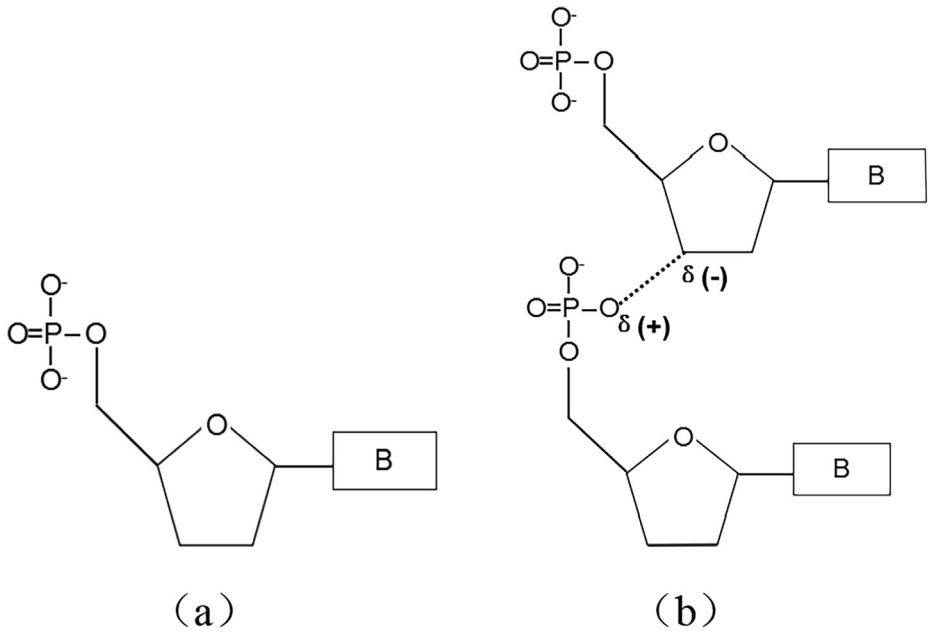

Fig. 1. The molecular structure of DNA (a: the molecular structure of a deoxynucleoside, b: the molecular structure of an oligonucleotide).

Table 2
Configuration scheme for simulated concrete pore solutions.

Solution number	Corrosion system
C	SCP solution
A_0	SCP solution + 4% DNA
B_0	SCP solution + 4% P
A_1	SCP solution + 4% DNA + 0.02 mol/L Na_2SO_4
A_2	SCP solution + 4% DNA + 0.05 mol/L Na_2SO_4
A_3	SCP solution + 4% DNA + 0.10 mol/L Na_2SO_4
B_1	SCP solution + 4% P + 0.02 mol/L Na_2SO_4
B_2	SCP solution + 4% P + 0.05 mol/L Na_2SO_4
B_3	SCP solution + 4% P + 0.10 mol/L Na_2SO_4

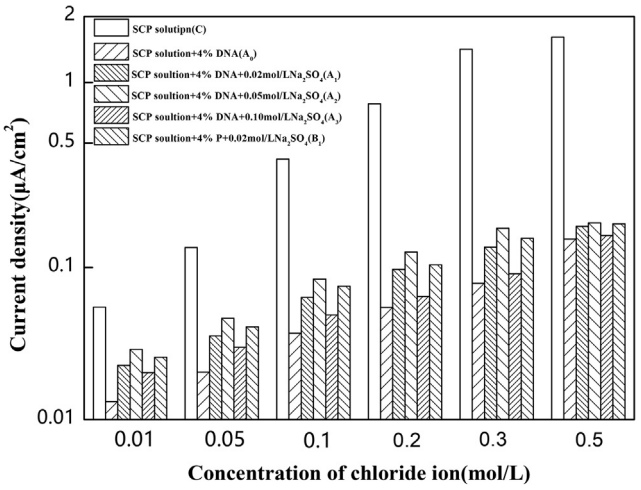

Fig. 2. Corrosion current density of different samples as a function of NaCl concentrations.

concentrations of Na_2SO_4. Then, DNA corrosion inhibitor (designated as DNA) and phosphate corrosion inhibitor (designated as P), both fixed at 4% (v/v), were added in these different types of SCP solutions. The control SCP solution (without both inhibitors and Na_2SO_4) was also prepared for comparison. Table 2 gives the composition of different SCP solutions. Cl^- (as NaCl) was introduced into the above SCP solutions step by step in gradient (0.01 mol/L per day) until all the reinforced steels were corroded.

2.3. Characterization

Changes in the electrochemical properties of reinforced steels in SCP solutions were monitored by linear polarization resistance and EIS. The electrochemical experiments were performed using a PARSTAT 2273 electrochemical workstation. The common three-electrode system was adopted, with the reinforced steel acting as the working electrode, a saturated calomel electrode (SCE) serving as the reference electrode and a platinum electrode functioning as the counter electrode. After the open circuit potential (OCP) of the working electrode was stable, the electrochemical tests were conducted immediately at room temperature. The linear polarization resistance tests were performed within the potential range of from −15 mV to +15 mV vs. OCP with a scan rate of 0.2 mV/s and the EIS measurements were carried out in a frequency range from 100 KHz to 10 mHz. The chemical compositions of the formed passive films of the steel electrodes treated by the DNA corrosion inhibitor were analyzed using XPS (Thermo ESCALAB 250XI).

3. Results and discussion

3.1. Electrochemical behavior of reinforced steel

3.1.1. Linear polarization resistance

Due to the small scanning range of linear polarization, the measured curve of E-I can be approximate to a straight line. Therefore, the reinforced electrode polarization resistance (R_p) can be represented by the slope of the line [37]. Based on the Stern-Geary theory, the corrosion current (I_{corr}) can be calculated by Eq. (1). Since the corrosion rate of the reinforced steel is related to the surface area of the steel electrode, using corrosion current density (i_{corr}) rather than the corrosion current describes the corrosion more accurately. The corrosion current density can be calculated by Eq. (2). The results of each group treated by different concentrations of NaCl are shown in Fig. 2.

$$I_{corr} = \frac{B}{R_p} \tag{1}$$

$$i_{corr} = \frac{I_{corr}}{A} \tag{2}$$

where A is the surface area of steel electrode (which was 0.785 cm^2 in this study), and B is the Stern-Geary constant related to the testing system (for the embedded reinforced steel in concrete, B is 26 mV when the steel electrode is in the corrosion state, and 52 mV when it is in the passive state [4,38]).

According to the published literatures [39,40], the corrosion rate of reinforced steel can be grouped into four levels: passive condition (i_{corr} < 0.1 μA/cm^2), low to moderate corrosion condition (0.1 μA/cm^2 < i_{corr} < 0.5 μA/cm^2), moderate to high corrosion condition (0.5 μA/cm^2 < i_{corr} < 1 μA/cm^2) and high corrosion condition (i_{corr} > 1 μA/cm^2). At a concentration of 0.01 mol/L NaCl, the corrosion current density (i_{corr}) of all the samples was below 0.10 μA/cm^2, indicating that the steel electrode was in the passivation state (Fig. 2). The current density of the blank sample C was the highest. Meanwhile, the corrosion current density of the DNA corrosion inhibitor incorporated samples containing different SO_4^{2-} concentrations was in the decreasing order of $A_2 > B_1 > A_1 > A_3$. When the NaCl concentration was elevated to 0.05 mol/L, the i_{corr} of the blank sample C was higher than 0.10 μA /cm^2, pointing to the corrosion state. It was noteworthy that even when the blank sample C evolved to the mild corrosion state, all the DNA corrosion inhibitor incorporated samples still remained in the passive state. The same was true when the NaCl concentration was 0.01 mol /L.

As the NaCl concentration was further increased to 0.20 mol/L, the blank sample C was in the moderate corrosion state (0.50 μA/cm^2 < i_{corr} < 1 μA/cm^2). The A_2 sample was in a slightly corrosive state, while both B_1 and A_1 was in a state of close to corrosion. It should also be noted that the differences in the corrosion current density between A_3 and A_0 narrowed. At a NaCl concentration of 0.3 mol/L, the blank sample C entered the severe corrosion stage (i_{corr} > 1 μA/cm^2). In contrast, B_1 and A_1 were still in a slight corrosion state, while A_3 and A_0 were still in the passive state. Furthering increasing the NaCl concentration to 0.5 mol/L transformed A_3

Table 3
Steel electrode corrosion resistant efficiency in each corrosion pool tested by linear polarization (%).

Corrosion system	0.01 mol/L NaCl	0.05 mol/L NaCl	0.10 mol/L NaCl	0.20 mol/L NaCl	0.30 mol/L NaCl	0.50 mol/L NaCl
SCP solution + 4%DNA (A_0)	76.37	83.71	90.60	92.79	94.41	90.92
SCP solution + 4%DNA + 0.02 mol/L Na_2SO_4 (A_1)	58.19	71.68	84.06	87.61	90.77	89.25
SCP solution + 4%DNA + 0.05 mol/L Na_2SO_4 (A_2)	46.61	63.27	79.30	84.26	88.11	88.71
SCP solution + 4%DNA + 0.10 mol/L Na_2SO_4 (A_3)	62.55	76.22	87.67	91.57	93.60	90.47
SCP solution + 4%P + 0.02 mol/L Na_2SO_4 (B_1)	52.74	67.57	81.33	86.83	89.60	88.88
SCP solution (C)	–	–	–	–	–	–

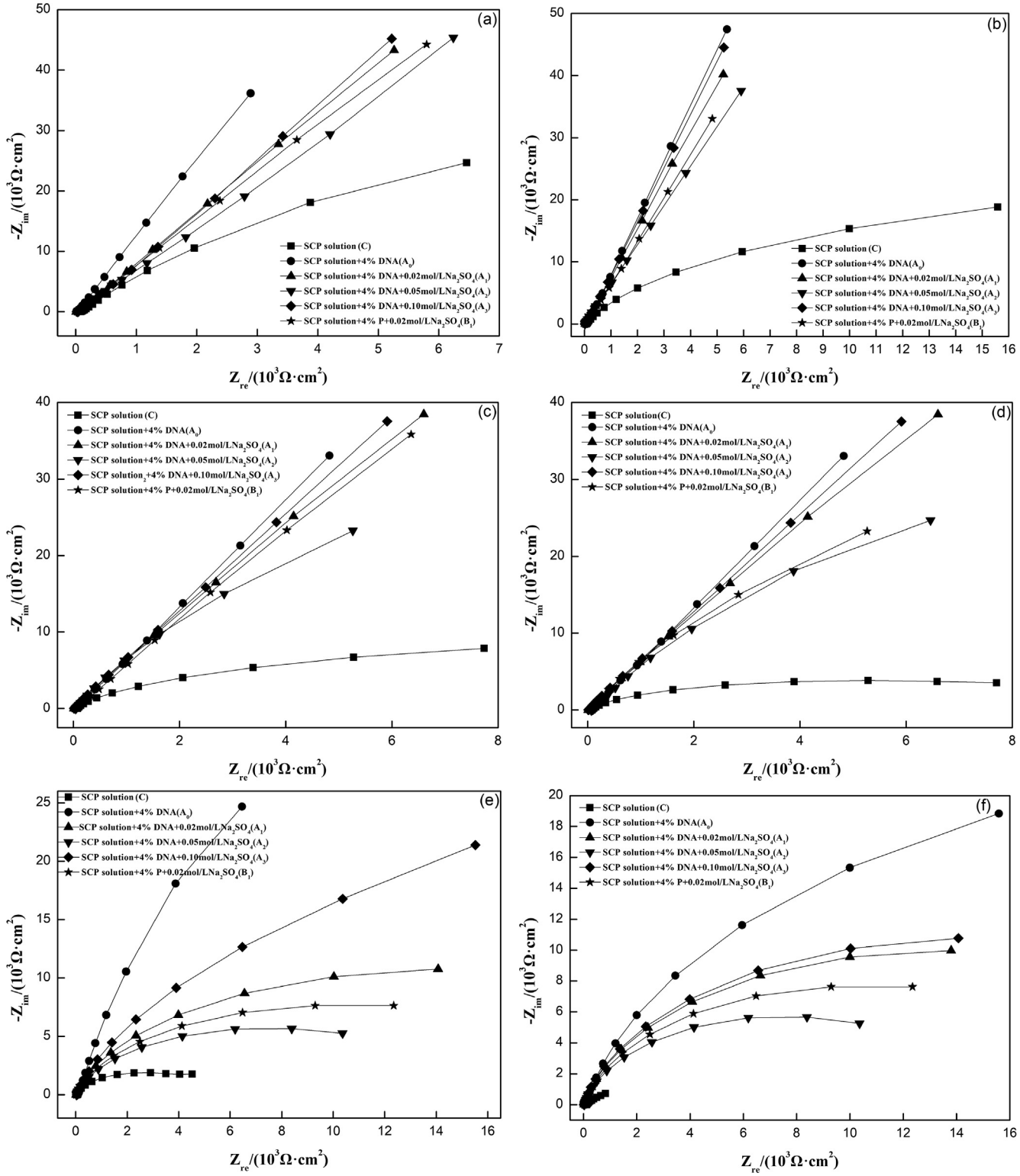

Fig. 3. Nyquist plot of different samples in the presence of different concentrations of NaCl (a: 0.01 mol/L NaCl, b: 0.05 mol/L NaCl, c: 0.10 mol/L NaCl, d: 0.20 mol/L NaCl, e: 0.30 mol/L NaCl, f: 0.50 mol/L NaCl).

and A_0 into the mild corrosion state ($i_{corr} > 0.10$ μA/cm^2). The corrosion state of other samples remained the same as that of those at a NaCl concentration of 0.30 mol/L despite a slight increase in the corrosion current density.

Corrosion resistant efficiency can be used to more clearly reflect the corrosion resistant effect of DNA, which can be calculated by Eq. (3).

$$\eta = \frac{i_0 - i_1}{i_0} \tag{3}$$

where η is the corrosion resistance efficiency for arbitrary system 1, i_0 is the corrosion current density of blank, and i_1 is the corrosion current density of arbitrary system 1.

As can be seen from Table 3, the addition of the DNA corrosion inhibitors had a positive effect on inhibiting the corrosion of rein-

forced electrode. However, the corrosion resistant efficiency of DNA corrosion inhibitors was reduced under the coexistence of SO_4^{2-} and Cl^-. Interestingly, increasing the concentration of SO_4^{2-} from 0.05 mol/L to 0.10 mol/L led to an accompanying increase in the corrosion resistant efficiency of DNA corrosion inhibitors. It can also be observed that with the increase of NaCl concentration, the effect of SO_4^{2-} on the corrosion resistance of DNA corrosion inhibitor and commercial corrosion inhibitor was smaller and less. For example, with the treatment of 0.50 mol/L NaCl, the difference in the corrosion inhibiting efficiency between the samples exposed to A_3 (with 0.1 mol/L SO_4^{2-}) and those exposed to A_0 (without SO_4^{2-}) was only about 5%.

3.1.2. EIS

Fig. 3(a) and (b) provide the EIS of different samples in the presence of 0.01 mol/L and 0.05 mol/L NaCl, respectively. At a lower concentration of NaCl (0.01 mol/L), all the samples had a slightly low frequency curve, but their overall radius was bigger, indicating that the polarization resistance was not significantly reduced. When the concentration of NaCl was further increased to 0.05 mol/L, the reinforced electrode treated by DNA corrosion inhibitors still remained passivation. In stark contrast, the polarization resistance of the blank sample C steel was significantly reduced, suggesting that the steel entered a state of corrosion.

Fig. 3(c) and (d) respectively provides the EIS of different samples in the presence of 0.10 mol/L and 0.20 mol/L NaCl. When 0.20 mol/L NaCl was added, the radius of the C, A_2 and B_1 curves significantly decreased, reflecting a significant decrease in their polarization resistance and thereby a shift from the passivation state to the corrosion state. In contrast, the radius of the A_0 (with only DNA corrosion inhibitor) curves was still relatively large, indicating an effective corrosion inhibition induced by the DNA corrosion inhibitor. However, the presence of SO_4^{2-} adversely reduced the corrosion inhibitor efficiency of the DNA corrosion inhibitor. It is noteworthy that the low-frequency curve radius of A_1 was larger than that of B_1 (containing the commercial corrosion inhibitor) subjected to the Cl^- and SO_4^{2-} coexisting environments at the same concentration, indicating that the DNA corrosion inhibitor possessed a higher corrosion inhibitor efficiency compared with the commercial corrosion inhibitor. Meanwhile, the largest curve radius of A_3 pointed to the highest corrosion inhibitor efficiency of the DNA corrosion inhibitor with exposure to 0.02 mol/L SO_4^{2-}.

Fig. 3(e) and (f) gives the EIS of different samples after exposure to 0.30 mol/L and 0.50 mol/L NaCl, respectively. Apparently, the curve radius of all the samples further decreased. The curve radius of the samples was in the decreasing order of is $A_3 > A_1 > A_2$. It can also be seen that with the addition of 0.10 mol/L SO_4^{2-}, the DNA corrosion inhibitor delivered the best corrosion inhibitor effect.

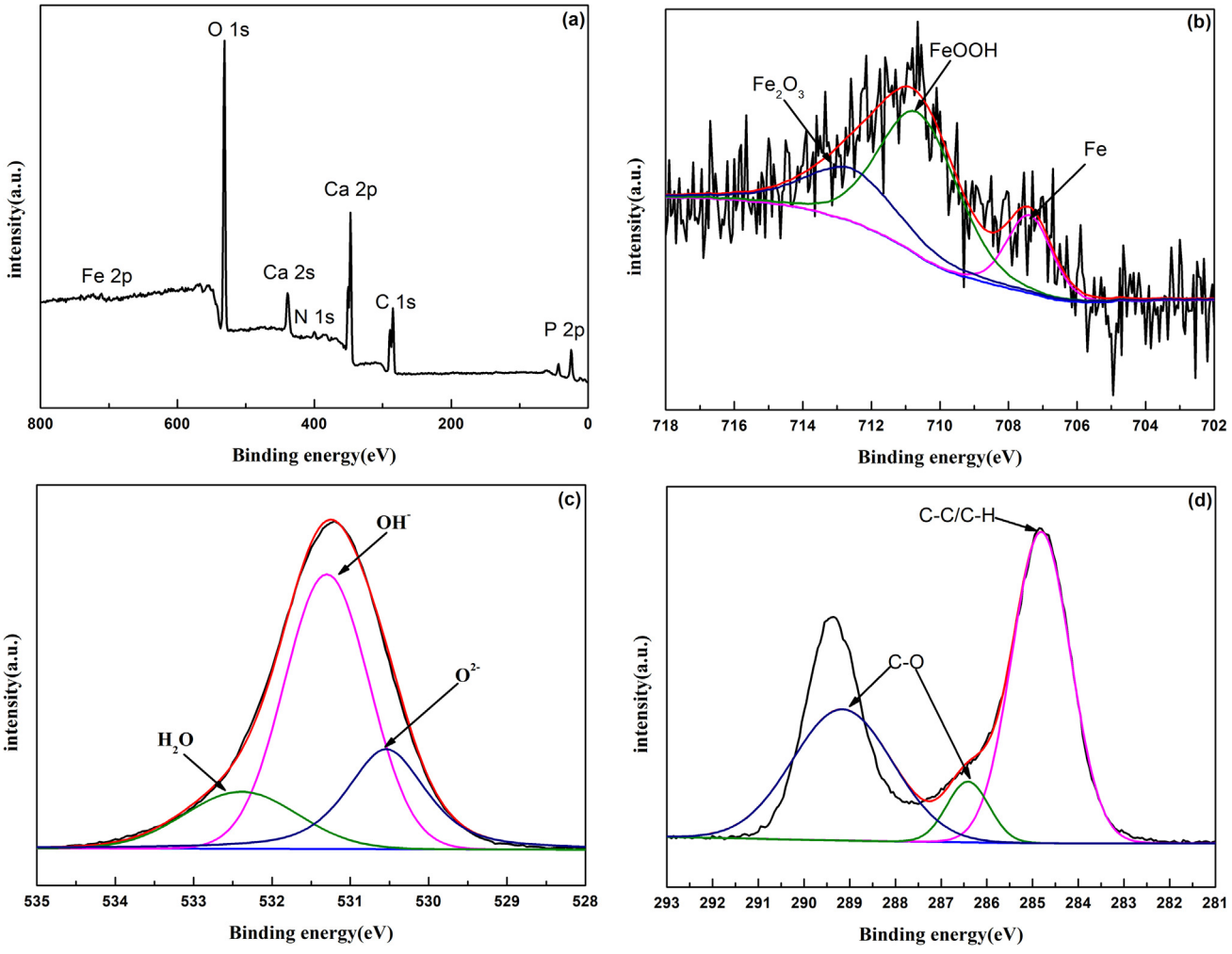

Fig. 4. XPS spectra of reinforced steel after immersed in SCP solution in the presence of 4% DNA for 7 days. (a: wide-scan spectra, b: Fe 2p spectra, c: O 1s spectra, and d: C 1s spectra).

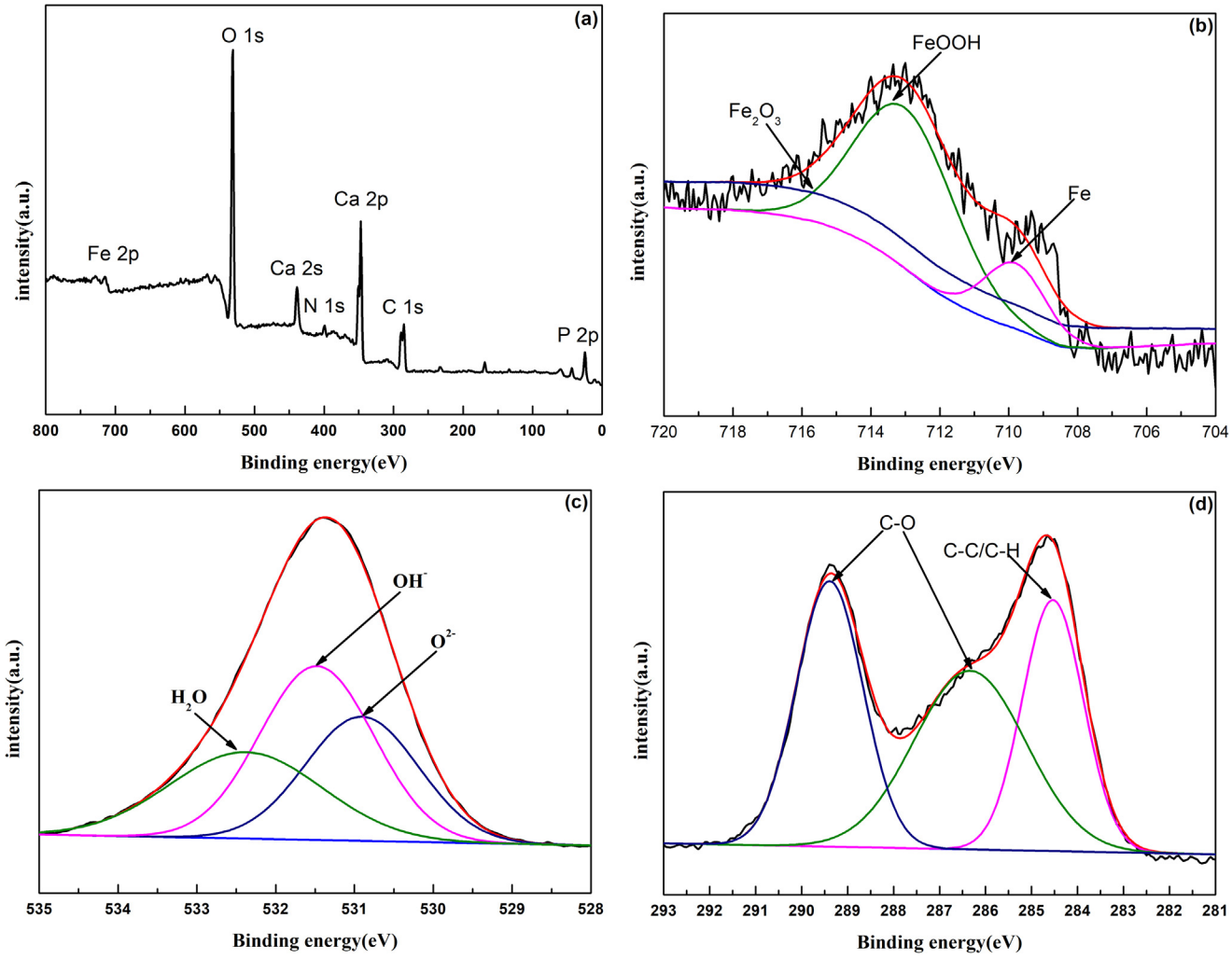

Fig. 5. XPS spectra of reinforced steel after immersed in SCP solution in the presence of 4% DNA and 0.10 mol/L Na_2SO_4 for 7 days. (a: wide-scan spectra, b: Fe 2p spectra, c: O 1s spectra, and d: C 1s spectra).

B_1 and A_1 was in the corrosion state, while A_3 was still in the passivation state. Fig. 3(f) demonstrated that all the samples were corroded (reflected by a significantly reduced curve radium). This observation meant that the corrosion inhibitor effect of both the DNA and commercial corrosion inhibitors suffered from a significant reduction in the corrosion inhibition efficiency.

As can be seen from Fig. 3, when the concentration of SO_4^{2-} was low (from 0.02 mol/L to 0.05 mol/L), the addition of SO_4^{2-} to the Cl^- containing SCP reduced the corrosion inhibition efficiency of DNA corrosion inhibitor. Conversely, when the concentration of SO_4^{2-} was high (from 0.05 mol/L to 0.10 mol/L), the presence of SO_4^{2-} (in the presence of SO_4^{2-} to Cl^-) reduced the corrosion rate of steel reinforcement, improved the corrosion inhibition efficiency of DNA corrosion inhibitor, and, to some extent, inhibited the corrosion of chloride in reinforced steel. This may be due to the competing adsorption of SO_4^{2-} and Cl^- on the surface of the reinforcement. Because SO_4^{2-} has two negative charges, it has better nucleophilicity than Cl^-. Therefore, under SO_4^{2-} and Cl^- coexisting conditions, increasing SO_4^{2-} concentration led to the replacement of Cl^- on the surface of reinforcement through competing adsorption. As a result, the content of Cl^- on the surface of reinforcement was reduced, thereby inhibiting the corrosion of reinforcement.

3.2. XPS

XPS analysis was carried out to study the surface composition of the DNA corrosion inhibitors treated reinforced steel immersed in various Cl^- and SO_4^{2-} coexisting environments. The XPS analysis results are shown in Figs. 4 and 5. Figs. 4(a) and 5(a) provide the wide-scan XPS spectra of the reinforced steel. Fe, O, C, Ca, N and P were the main observed elements with the presence of a small amount of other elements. The five basic elements of DNA molecules were all detected (O 1s, N 1s, Fe 2p, C 1s, and P 2p). The presence of Ca element may be due to the deposition of $Ca(OH)_2$ on the passivation film of the steel surface.

The XPS spectra of C 1s, Fe 2p and O 1s of the reinforced steel after immersed in SCP solution in the presence of 4% DNA for 7 days are presented in Fig. 4(b), Fig. 4(c) and Fig. 4(d), respectively. After immersed in SCP solution in the presence of 4% DNA and 0.10 mol/L Na_2SO_4 for 7 d, their corresponding XPS spectra of C 1s, Fe 2p and O 1s are presented in Fig. 5(b), Fig. 5(c) and Fig. 5(d), respectively. The Fe 2p photoelectron peaks at 707.4, 710.6 and 712.6 eV, and the characteristic binding energies at 710.4 eV correspond to FeOOH, while the photoelectron peak at 712.6 eV corresponds to Fe_2O_3 [41,42] (as shown in Fig. 4(b)). The emerge of typical Fe_2O_3 peaks clearly pointed to the oxidization of the

Table 4
Relative strength of corrosion systems (%).

Corrosion system	FeOOH	Fe_2O_3	C-O
SCP solution + 4%DNA (A_0)	36.39	42.66	70.77
SCP solution + 4%DNA + 0.10 mol/L Na_2SO_4 (A_3)	81.13	11.65	74.51

steel, which formed a layer of passive films on the steel surface. Similarly, in Fig. 5(b), the Fe 2p photoelectron peaks at 709.8, 713.0 and 716.7 eV, and the characteristic binding energies at 713.0 eV correspond to FeOOH, while the photoelectron peak at 716.7 eV corresponds to Fe_2O_3, exhibiting similar features and peak positions to the blank sample. The binding energy at 707.4 eV and 709.8 eV corresponds to Fe [43] (as shown in Fig. 4 (b) and Fig. 5(b)). It can be seen from Fig. 4(c) that the O 1s pattern was decomposed into three peaks: O^{2-} at 530.5 eV, the adsorption of H_2O at 532.4 eV, and OH^- at 531.3 eV. These coincided with the Fe 2p spectrum of iron hydroxide layer. Meanwhile, the C 1s pattern was also decomposed into three peaks: C—C or C—H at 284.8 eV, C—O at 286.4 eV and 289.2 eV [44] (as shown in Fig. 4 (c) and (d)). It can be seen from Fig. 5(c) and (d) that the peak value only changed slightly, and their content changed correspondingly (as shown in Table 4). The overall results demonstrated that an adsorption film was formed on the reinforced steel.

Through the XPS analysis, the corrosion inhibiting mechanisms of the DNA inhibitor can be deduced as follows: In the early stage of corrosion, the phosphate (with a strong electron donor capacity) in the DNA corrosion inhibitor bonds with the d vacant orbital of Fe, thus effectively inhibiting the adsorption of coexisting anions SO_4^{2-} and Cl^- on the surface of reinforced steel. In the later stage, the effect of coexisting SO_4^{2-} on the corrosion inhibition of both the DNA corrosion inhibitors and the commercial corrosion inhibitors was attenuated. With the increase of the Cl^- content, Cl^- replaced SO_4^{2-} as the main adsorption ion through competing adsorption. Meanwhile, the corrosion inhibitor was consumed continuously, and the film covering the surface of the reinforcement was destroyed gradually. As a result, the DNA corrosion inhibitor can only be adsorbed on the areas where the electrode reaction was more active, causing pitting corrosion.

The qualification-quantification analysis of the recorded XPS spectra of the product layer was performed, and the results are shown in Table 4. After the addition of SO_4^{2-}, the content of FeOOH in the passivation film increased from 36.39% to 81.13%, while the content of C-O increased from 70.77% to 74.51%. These changes pointed to an increase in the corrosion products on the reinforced steel surface, thereby resulting in an increase in the content of the outer membrane. Whereas, the content of Fe_2O_3 decreased by 31.01%, indicating that the internal denser membrane structure became looser, the corrosion resistance of reinforced steel surface passivation film was reduced, and the corrosion rate of reinforced steel increased. Collectively, these findings clearly demonstrated that the addition of SO_4^{2-} reduced the corrosion resistant effect of the DNA corrosion inhibitors.

4. Conclusions

Based on the findings from this study, the following conclusions can be drawn:

(a) The presence of low concentration (0.02 mol/L) SO_4^{2-} in the Cl^- abundant environment adversely reduced the corrosion inhibitor efficiency of the DNA corrosion inhibitor, while the presence of high concentration (0.10 mol/L) SO_4^{2-} had a negligible effect on the corrosion inhibitor efficiency of the DNA corrosion inhibitor in the same environment. This conclusion was corroborated by linear polarization and by electrochemical impedance spectroscopy (EIS), as well as by the XPS analysis.

(b) The efficiency of the adopted DNA corrosion inhibitor was higher than that of a typical commercial corrosion inhibitor (sodium phosphate) under the same condition (at 0.02 mol/L SO_4^{2-}). In addition, at 0.10 mol/L SO_4^{2-}, the corrosion inhibitor efficiency of the DNA corrosion inhibitor was the highest.

(c) With the increase of NaCl concentration, the effect of SO_4^{2-} on the corrosion resistance of DNA corrosion inhibitor and commercial corrosion inhibitor was smaller and less. When the NaCl concentration was increased to 0.50 mol/L, the difference in corrosion inhibitor efficiency between the DNA corrosion inhibitors treated samples subjected to 0.1 mol/L SO_4^{2-} and those without SO_4^{2-} was only about 5%.

Declaration of Competing Interest

The authors have declared that no conflict of interest exists.

Acknowledgment

The authors wish to thank the National Key R&D Program of China (2018YFC1508704), the Fundamental Research Funds for the Central Universities (2018B692X14), the Postgraduate Research & Practice Innovation Program of JiangSu Province (KYCX18_0571) and the China Postdoctoral Science Foundation (2018M632219) for funding support.

References

[1] K.A.A. Al-Sodani, M. Maslehuddin, O.S.B. Al-Amoudi, T.A. Saleh, M. Shameem, Efficiency of generic and proprietary inhibitors in mitigating Corrosion of Carbon Steel in Chloride-Sulfate Environments, Sci. Rep.-UK 8 (1) (2018).
[2] S.A. Asipita, M. Ismail, M.Z.A. Majid, Z.A. Majid, C.S. Abdullah, J. Mirza, Green Bambusa Arundinacea leaves extract as a sustainable corrosion inhibitor in steel reinforced concrete, J. Clean. Prod. 67 (6) (2014) 139–146.
[3] J. Cai, C. Chen, J. Liu, J. Liu, Corrosion resistance of carbon steel in simulated concrete pore solution in presence of 1-dihydroxyethylamino-3-dipropylamino-2-propanol as corrosion inhibitor, Br. Corros. J. 49 (1) (2014) 66–72.
[4] Shamsad Ahmad, Reinforcement corrosion in concrete structures, its monitoring and service life prediction: a review, Cement Concrete Comp. 25 (4) (2003) 459–471.
[5] G.S. Duffó, S.B. Farina, C.M. Giordano, Characterization of solid embeddable reference electrodes for corrosion monitoring in reinforced concrete structures, Electrochim. Acta 54 (3) (2009) 1010–1020.
[6] L. Dhouibi, E. Triki, A. Raharinaivo, The application of electrochemical impedance spectroscopy to determine the long-term effectiveness of corrosion inhibitors for steel in concrete, Cement Concrete Comp. 24 (1) (2002) 35–43.
[7] G.K. Glass, N.R. Buenfeld, The influence of chloride binding on the chloride induced corrosion risk in reinforced concrete, Corros. Sci. 42 (2) (2000) 329–344.
[8] P. Garcés, P. Saura, E. Zornoza, C. Andrade, Influence of pH on the nitrite corrosion inhibition of reinforcing steel in simulated concrete pore solution, Corros. SCI. 53 (12) (2011) 3991–4000.
[9] Z.L. Cao, H.Y. Chen, L.Y. Wei, M. Hibino, Effect of anodic and cathodic chloride contents on the macrocell corrosion and polarization behavior of reinforcing steel, Int. J. Eng. Res. Afr. 22 (2016) 45–58.
[10] M. Criado, I. Sobrados, J.M. Bastidas, J. Sanz, Steel corrosion in simulated carbonated concrete pore solution its protection using sol–gel coatings, Prog. Org. Coat. 88 (2015) 228–236.
[11] J. Xu, L. Jiang, F. Xing, Influence of N,N′-dimethylaminoethanol as an inhibitor on the chloride threshold level for corrosion of steel reinforcement, Mater. Corros. 61 (9) (2015) 802–809.
[12] B.S. Liu, D.W. Yang, L.X. Zhong, Z. Feng, Research on effects of inhibitors on anti-corrosion performance of reinforced bar in the concrete, Adv. Mater. Res. 239–242 (2011) 1195–1198.
[13] T. Sugama, N.R. Carciello, Corrosion protection of steel and bond durability at polyphenylene sulfide-to-anhydrous zinc phosphate interfaces, J. Appl. Polym. Sci. 45 (7) (2010) 1291–1301.
[14] A. Królikowski, J. Kuziak, Impedance study on calcium nitrite as a penetrating corrosion inhibitor for steel in concrete, Electrochim. Acta 56 (23) (2011) 7845–7853.

[15] H.S. Ryu, J.K. Singh, H.M. Yang, H.S. Lee, M.A. Ismail, Evaluation of corrosion resistance properties of N, N′-Dimethyl ethanolamine corrosion inhibitor in saturated Ca(OH) 2 solution with different concentrations of chloride ions by electrochemical experiments, Constr. Build. Mater. 114 (2016) 223–231.
[16] V. Saraswathy, S. Muralidharan, R.M. Kalyanasundaram, Evaluation of a composite corrosion-inhibiting admixture and its performance in concrete under macrocell corrosion conditions, Cem. Concr. Res. 31 (5) (2001) 789–794.
[17] O.S.B. Al-Amoudi, M. Maslehuddin, A.N. Lashari, A.A. Almusallam, Effectiveness of corrosion inhibitors in contaminated concrete, Cement Concrete Comp. 25 (4) (2003) 439–449.
[18] H.S. Lee, H.S. Ryu, W.J. Park, M.A. Ismail, Comparative study on corrosion protection of reinforcing steel by using amino alcohol and lithium nitrite inhibitors, Materials 8 (1) (2015) 251.
[19] P. Garcés, P. Saura, A. Méndez, E. Zornoza, C. Andrade, Effect of nitrite in corrosion of reinforcing steel in neutral and acid solutions simulating the electrolytic environments of micropores of concrete in the propagation period, Corros. Sci. 50 (2) (2008) 498–509.
[20] J. Tritthart, Transport of a surface-applied corrosion inhibitor in cement paste and concrete, Cem. Concr. Res. 33 (6) (2003) 829–834.
[21] F.L. Fei, H. Jie, J.X. Wei, Q.J. Yu, Z.S. Chen, Corrosion performance of steel reinforcement in simulated concrete pore solutions in the presence of imidazoline quaternary ammonium salt corrosion inhibitor, Constr. Build. Mater. 70 (2014) 43–53.
[22] S. Jiang, L. Jiang, Z. Wang, M. Jin, S. Bai, S. Song, et al., Deoxyribonucleic acid as an inhibitor for chloride-induced corrosion of reinforcing steel in simulated concrete pore solutions, Constr. Build. Mater. 150 (2017) 238–247.
[23] S. Jiang, G. Song, L. Jiang, M.Z. Guo, J. Yu, C. Chen, et al., Effects of Deoxyribonucleic acid on cement paste properties and chloride-induced corrosion of reinforcing steel in cement mortars, Cement Concrete Comp. 91 (2018) 87–96.
[24] J. Zhou, X. Chen, S. Chen, Durability and service life prediction of GFRP bars embedded in concrete under acid environment, Nucl. Eng. Des. 241 (10) (2011) 4095–4102.
[25] Q.F. Xu, W. Wang, X.L. Pang, Q.L. Liu, K.W. Gao, Investigation of corrosion behaviours of high level waste container materials in simulated groundwater in China, Br. Corros. J. 49 (6) (2014) 480–484.
[26] H. Alwi, J. Idris, M. Musa, et al., A preliminary study of banana stem juice as a plant-based coagulant for treatment of spent coolant wastewater, J. Chem. 2013 (2) (2013) 1–7.
[27] C. Andrade, C. Alonso, Test methods for on-site corrosion rate measurement of steel reinforcement in concrete by means of the polarization resistance method, Mater. Struct. 37 (9) (2004) 623–643.
[28] H.X. Qiao, W. Gong, Q.Y. Cheng, J.M. Dong, G.F. Chen, L. Hua, Durability of magnesium cement reinforced concrete in saline soil area, J. China Coal Soc. (2015).
[29] F. Ming, Y.S. Deng, D.Q. Li, Mechanical and durability evaluation of concrete with sulfate solution corrosion, Adv. Mater. Sci. Eng. 2016 (4) (2016) 1–7.
[30] E. Smailos, W. Schwarzkopf, B.K.R. Köster, Corrosion of carbon-steel containers for heat-generating nuclear waste in brine environments relevant for A rock-salt repository, Mrs Proc. 257 (2011) 399.
[31] W.F. Jin, Y.H. Wang, G. Zhou, K. Fan, experimental study on anti-frozen durability of concrete in saline soil region, Adv. Mater. Res. 368–373 (2011) 6.
[32] N. Gartner, T. Kosec, A. Legat, The efficiency of a corrosion inhibitor on steel in a simulated concrete environment, Mater. Chem. Phys. 184 (2016) 31–40.
[33] F. Shaheen, B. Pradhan, Influence of sulfate ion and associated cation type on steel reinforcement corrosion in concrete powder aqueous solution in the presence of chloride ions, Cem. Concr. Res. 91 (2017).
[34] H.X. Qiao, Z.W. Zhang, S. Gao, H. Mao, S.Q. Liu, Electrochemical corrosion behavior of reinforcing steel in coupling environment of sulphate with chloride, J. Lanzhou Univ. Technol. (2017).
[35] M.A. Deyab, S.T. Keera, Cyclic voltammetric studies of carbon steel corrosion in chloride-formation water solution and effect of some inorganic salts, Egypt. J. Pet. 21 (1) (2012) 31–36.
[36] D. Fologea, M. Gershow, B. Ledden, D.S. Mcnabb, J.A. Golovchenko, J. Li, Detecting single stranded DNA with a solid state nanopore, Nano Lett. 5 (10) (2005) 1905–1909.
[37] R. Solmaz, E.A. Şahin, A. Döner, G. Kardaş, The investigation of synergistic inhibition effect of rhodanine and iodide ion on the corrosion of copper in sulphuric acid solution, Corros. Sci. 53 (10) (2011) 3231–3240.
[38] M.F. Montemor, A.M.P. Simoes, M.G.S. Ferreira, Chloride-induced corrosion on reinforcing steel: from the fundamentals to the monitoring techniques, Cement Concrete Comp. 25 (4) (2003) 491–502.
[39] L. Freire, M.A. Catarino, M.I. Godinho, M.J. Ferreira, M.G.S. Ferreira, A.M.P. Simões, et al., Electrochemical and analytical investigation of passive films formed on stainless steels in alkaline media, Cement Concrete Comp. 34 (9) (2012) 1075–1081.
[40] G.S. Duffó, S.B. Farina, C.M. Giordano, Embeddable reference electrodes for corrosion monitoring of reinforced concrete structures, Mater. Corros. 61 (6) (2015) 480–489.
[41] F.L. Fei, J. Hu, Q.J. Yu, J.X. Wei, Y.B. Nong, The effect of a tailored electro-migrating corrosion inhibitor on the corrosion performance of chloride-contaminated reinforced concrete, Mater. Corros. 66 (10) (2015) 1039–1050.
[42] A.P. Grosvenor, B.A. Kobe, M.C. Biesinger, N.S. Mcintyre, Investigation of multiplet Splitting of Fe 2p XPS spectra and bonding in iron compounds, Surf. Interface Anal. 36 (12) (2004) 1564–1574.
[43] L. Ming, X. Cheng, X. Li, J. Zhu, H. Liu, Corrosion behavior of Cr modified HRB400 steel rebar in simulated concrete pore solution, Constr. Build. Mater. 93 (2015) 884–890.
[44] A. Fedorkova, R. Orinakova, A. Orinak, M. Kupkova, H.D. Wiemhöfer, J.N. Audinot, et al., Electrochemical and XPS study of $LiFePO_4$ cathode nanocomposite with PPy/PEG conductive network, Solid State Sci. 14 (8) (2012) 1238–1243.